Depth and lateral resolution of laser-assisted atom probe microscopy of silicon revealed by isotopic heterostructures

Y. Shimizu,[1,a)] Y. Kawamura,[1] M. Uematsu,[1] M. Tomita,[2] T. Kinno,[2] N. Okada,[3] M. Kato,[3] H. Uchida,[3] M. Takahashi,[3] H. Ito,[4] H. Ishikawa,[4] Y. Ohji,[4] H. Takamizawa,[5] Y. Nagai,[5] and K. M. Itoh[1,b)]

[1]*School of Fundamental Science and Technology, Keio University, 3-14-1 Hiyoshi, Kohoku-ku, Yokohama 223-8522, Japan*
[2]*Corporate Research and Development Center, Toshiba Corporation, 8 Shinsugita-cho, Isogo-ku, Yokohama 235-8522, Japan*
[3]*Practical Analysis Technology Center, Toshiba Nanoanalysis Corporation, 1 Komukai Toshiba-cho, Saiwai-ku, Kawasaki 212-8583, Japan*
[4]*Selete, 16-1 Onogawa, Tsukuba, Ibaraki 305-8569, Japan*
[5]*The Oarai Center, Institute for Materials Research, Tohoku University, 2415-2 Narita, Oarai, Higashi-Ibaraki-gun, Ibaraki 311-1313, Japan*

(Received 17 November 2010; accepted 13 December 2010; published online 4 February 2011)

We report on a direct comparison of the depth and lateral resolution of the current state-of-the-art laser-assisted atom probe microscopy analysis of single-crystalline silicon. The isotopic heterostructures composed of 5–15 nm-thick ^{28}Si- and ^{30}Si-enriched layers were measured to reconstruct three-dimensional images of ^{28}Si and ^{30}Si stable isotope distributions in the surface perpendicular and parallel directions for the analysis of the depth and lateral resolution, respectively. The decay length experimentally obtained for the lateral direction is only about twice longer than in the direction, meaning that the lateral resolution is higher than obtained by secondary ion mass spectrometry. © *2011 American Institute of Physics*. [doi:10.1063/1.3544496]

With the rapid shrinkage of silicon (Si) based metal-oxide-semiconductor field-effect-transistors (FETs) and advancement of the three-dimensional (3D) structures like fin-FETs, 3D mapping of dopant distributions in Si with subnanometer scale becomes important for the precise identification of source and drain regions.[1] Laser-assisted atom probe microscopy[2–5] has been attracting much attention as a practical characterization technique that allows such 3D mapping.[6–8] The spatial resolution of the atom probe for Si in the direction parallel to the needle-shaped probe, hereafter depth resolution, is proven much higher than that of secondary ion mass spectrometry (SIMS),[9,10] and in the favorable case, individual (111) atomic plane can be resolved.[11] In general, the resolution of the direction perpendicular to the needle, hereafter lateral resolution, is expected to degrade due to surface migration of atoms in the atomic plane prior to their evaporation.[12] Heating and excitation due to the laser-irradiation may also enhance such in-plane migration. However, the potential for self-migration of Si on Si surface might be very low due to the nature of the bonding in Si. In addition, trajectory aberrations are the one of the reasons for lateral resolution degradation as reported in Refs. 13–15. Therefore, quantitative evaluation of the lateral resolution by the present atom probe is of great interest to clarify the reasons in host Si substrates while the in-depth resolution for Si was reported.[11] The present paper reveals the lateral resolution quantitatively with respect to the depth resolution using Si isotopic heterostructures based on the so-called decay lengths of the ^{28}Si and ^{30}Si concentration profiles around the interfaces of ^{28}Si/^{30}Si layers.

Si isotope heterostructures are the ideal samples for atom probe resolution measurements for the following reasons. The mass difference of ^{28}Si and ^{30}Si isotopes is large enough for the mass spectrometer to distinguish them with high fidelity but is small enough for ^{28}Si and ^{30}Si to exhibit the same diffusion, migration, and field evaporation behavior. Since the thickness of each isotopic layer is known from the growth condition, it can be used as the depth and/or lateral scale. For improving the 3D image reconstruction, the atomically flat interfaces between the adjacent isotopic layers can serve as the guideline for tuning the parameters such as radius of sample, field evaporation, etc. It is possible to take into account the change in hemispherical needle apex during the continuous evaporation of atoms.[16]

A detailed description of Si isotope heterostructures growth by solid-source molecular beam epitaxy is given elsewhere.[17,18] A high resistivity ($\rho > 2000\ \Omega$ cm), 2-in., *n*-type, (100)-oriented ^{nat}Si (^{28}Si:92.2 at. %, ^{29}Si:4.7 at. %, and ^{30}Si:3.1 at. %) wafer was employed as a substrate. A ^{nat}Si buffer layer of ~100 nm-thick was grown at 750 °C to form a smooth surface followed by the growth of alternating layers of enriched ^{28}Si and ^{30}Si at 650 °C. The isotopic heterostructure is composed of ^{30}Si(9 nm)/^{28}Si(5 nm)/^{30}Si(9 nm)/^{28}Si(5 nm)/^{30}Si(17 nm)/^{28}Si(10 nm)/^{30}Si(15 nm) from the top to bottom. This heterostructure is sandwiched by a ^{nat}Si buffer layer on the bottom and a ~20 nm-thick ^{nat}Si capping layer on the top. The intermixing at the ^{28}Si/^{30}Si interfaces is typically less than two atomic layers as revealed by Raman spectroscopy of confined optical phonons.[18,19] A laser-assisted local-electrode atom probe (LEAP) (LEAP3000XSi, Imago Scientific Instruments) with a green laser (wavelength: 532 nm) was employed. The detection efficiency was approximately 50%, which is consis-

[a)]Electronic mail: yshimizu@imr.tohoku.ac.jp.
[b)]Electronic mail: kitoh@appi.keio.ac.jp.

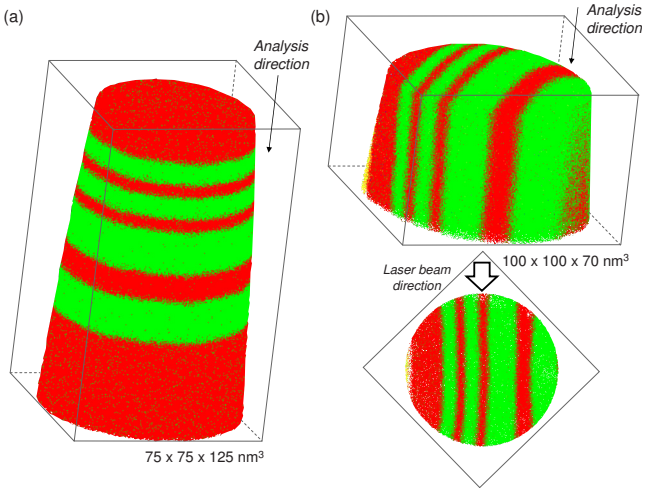

FIG. 1. (Color online) (a) 3D mapping of the isotopic heterostructures with the isotopic layers oriented perpendicular to the needle's long axis. Red and green dots represent ^{28}Si and ^{30}Si atoms, respectively. The reconstructed volume is $75\times75\times125$ nm^3. (b) 3D mapping of the isotopic heterostructures with the isotopic layers oriented parallel to the needle's long axis. Yellow dots represent Ni atoms which were deposited on top of the sample prior to Ga ion milling. The reconstructed volume is $100\times100\times70$ nm^3. The laser beam direction is shown in the top-view mapping.

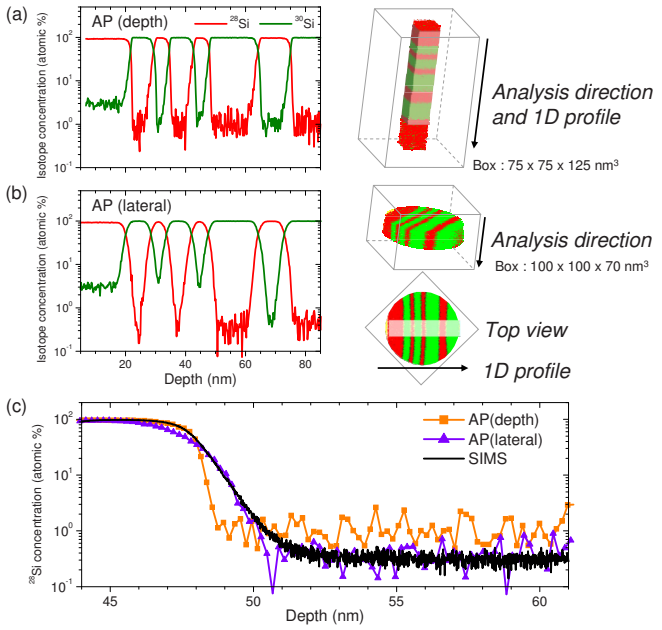

FIG. 2. (Color online) Depth profiles of ^{28}Si and ^{30}Si in the isotopic heterostructures analyzed along the (a) depth and (b) lateral directions by the atom probe. (c) Comparison of the profiles obtained by atom probe vertical and horizontal direction along with that determined by SIMS (O_2^+, 200 eV).

tent with the value of 55%–57% range using the similar LEAP system.[20] The laser pulse energy was 0.3 nJ. The base temperature of the sample was ~50 K to reduce surface migration.[12] The charge state ratio of $Si^+/Si^{2+}\sim10^{-3}$ is much smaller than those in the literature even for the equivalent pulse energy of 0.3 nJ, suggesting that in our experiment conditions were different compared to that reported in Ref. 16. For the depth resolution measurement, a ~30 nm-thick Ni protection layer was deposited on top of the ^{nat}Si capping layer before shaping of the sample into a needle by the Ga focused ion beam (FIB).[21] For the lateral resolution measurement, the same Ni layer was deposited on to the cross-sectional surface of the heterostructure and the needle was formed by FIB in the direction parallel to the heterostructure planes. 3D atom mapping images after the atom probe were reconstructed using the Imago Visualization and Analysis Software (IVAS) . Low-energy SIMS measurements (Cameca-SIMS4550) were performed to obtain the depth profiles of the isotopic heterostructures for comparison.

Figure 1(a) displays an example of a 3D mapping image of the isotope heterostructures for the analysis of depth resolution. ^{28}Si and ^{30}Si atoms are represented by red and green dots, respectively. The alternating layers of Si isotopes were clearly distinguished. However, clear visualization of (001) planes could not be achieved. Experimental conditions on, e.g., the sample temperature, laser energy, and pulsing can be optimal to obtain higher resolution. In addition, atomically flat interfaces of ^{28}Si/^{30}Si appear concaved, especially at the corner regions even after reconstruction. This artifact comes from the limitation in reconstructing the image based on the assumption that the surface remains perfectly hemispherical throughout the measurement. Recently, the actual reconstruction protocol implemented in IVAS is described in Ref. 22. Getting flat interfaces is a matter of adjusting the reconstruction parameters so as to obtain flat interfaces.[20,23] Acting on the initial radius while keeping the ratio of the field factor to image compression factor constant should change the curvature of the interface toward the edges of the field-of-view. In order to avoid the effect of the distortion, we select only the center region of the mapping image to obtain the depth profiles of ^{28}Si and ^{30}Si. Figure 1(b) shows an example of the atom probe image for the analysis of the lateral resolution. Regarding the distortions observed laterally at the corner part, they might originate from the slightly distorted radius of the needle during the continuous evaporation not from the protocol. Distortions in lateral planes cannot be corrected in the current protocol. This successful reconstruction obtained from the lateral direction shows that the periodic isotope layers can be employed as an absolute marker for lateral scaling calibration.

Figures 2(a) and 2(b) summarize the depth profiles of the ^{28}Si and ^{30}Si in the volume of $20\times20\times90$ nm^3 of the isotopic heterostructures obtained for the depth [Fig. 1(a)] and lateral [Fig. 1(b)] analyses, respectively. For comparison, SIMS profiles obtained with 200 eV O_2^+ primary ions are shown in Fig. 2(c). This SIMS measurement condition is found to be optimal for minimizing the atomic mixing by O_2^+ bombardment to achieve the highest depth resolution. Apparently, the atom probe profiles obtained by depth analysis show sharper interfaces than the one by SIMS. Here, quantitative evaluation of up- and down-slopes at the interfaces allows evaluation of the depth and lateral resolution.

Figure 3(a) shows the central part of the cross-section of Fig. 1(a). Figure 3(b) summarizes the decay lengths of ^{28}Si for the down-slope between the interface positions defined in Fig. 3(a). In this study, the slopes at each interface ^{28}Si/^{30}Si were determined from the ^{28}Si contents between 1% and 10%. As a result, a significant difference of the slopes, shown in Fig. 3(b), was observed. The mean decay lengths

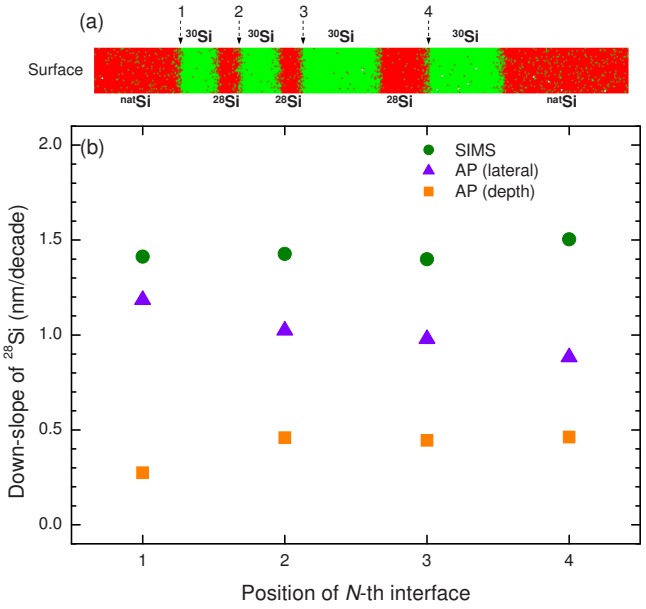

FIG. 3. (Color online) (a) Projected mapping image of ^{28}Si (red dots) and ^{30}Si (green dots) of the specimen. Each interface (*N*-th interface) is numbered for identification. (b) Down-slopes of ^{28}Si profiles in nanometer/decade as a function of the position of *N*-th interface. The squares, triangles, and circles represent down-slopes (decay lengths) of each interface obtained from atom probe depth, lateral direction, and SIMS, respectively.

obtained from depth, lateral, and SIMS were 0.4 nm/decade, 1.0 nm/decade, and 1.4 nm/decade, respectively. It has been demonstrated that the abruptness of ^{28}Si/^{30}Si interfaces is a few atomic monolayers (~0.3 nm)[18,19] and, therefore, the value of ~0.4 nm/decade obtained in the present atom probe represent the true profile, i.e., the actual resolution may be even better. The decay length for the depth direction is shorter than that for the lateral direction due to the existence of the surface migration prior to the field evaporation. Larger deviations from the mean value for the atom probe than those for SIMS can be consequence of the imperfection in the reconstructed images. This imperfection may come from the deviation from the hemispherical shape of the needle apex during evaporation. The in-plane distortion may be more serious for the analysis of the state-of-the-art nano Si devices since the straightedge guideline within the plane is more difficult to identify than the flat surface guideline that is naturally available for the vertical and horizontal direction analyses.

Finally, the decay length of SIMS is longer than that of atom probe even under low-energy conditions to minimize the artifact. Such isotopic heterostructures can be used as a reference sample for determination of depth resolution function of SIMS.[24] Depth resolution functions of SIMS have been evaluated by using boron-delta layers as markers embedded in Si substrates.[25,26] The decay lengths at the boron delta-layers strongly depend on Cs^+ or O_2^+ bombardment conditions. Ideally, a standard sample composed exclusively of Si, e.g., isotopic heterostructures, is desired to avoid the chemical effects such as migration of boron during Cs^+ or O_2^+ bombardments. Using the depth concentration profile of Si isotopes determined by the atom probe as a standard, SIMS mixing that depends on the primary ion species, incident angle, etc.[27] can be quantitatively evaluated.

In summary, the isotopic distribution in ^{28}Si/^{30}Si isotopic heterostructures composed of a stack of the 5–15 nm-thick stable isotope layers was evaluated by laser-assisted atom probe and a direct comparison between the depth and lateral directions was performed. The average decay length obtained from the lateral direction is only twice as degraded as that obtained from the depth direction, and is still shorter than the decay length of the profile measured by SIMS.

This work was supported in part by Grant-in-Aid for Scientific Research by MEXT, in part by Special Coordination Funds for Promoting Science and Technology, in part by FIRST, and in part by a Grant-in-Aid for the Global Center of Excellence at Keio University.

[1]International Technology Roadmap for Semiconductors 2009 edition, Metrology, http://www.itrs.net/
[2]B. Gault, F. Vurpillot, A. Vella, M. Gilbert, A. Menand, D. Blavette, and B. Deconihout, Rev. Sci. Instrum. **77**, 043705 (2006).
[3]T. F. Kelly and M. K. Miller, Rev. Sci. Instrum. **78**, 031101 (2007).
[4]T. F. Kelly, D. J. Larson, K. Thompson, R. L. Alvis, J. H. Bunton, J. D. Olson, and B. P. Gorman, Annu. Rev. Mater. Res. **37**, 681 (2007).
[5]D. N. Seidman and K. Stiller, MRS Bull. **34**, 717 (2009).
[6]K. Inoue, F. Yano, A. Nishida, H. Takamizawa, T. Tsunomura, Y. Nagai, and M. Hasegawa, Ultramicroscopy **109**, 1479 (2009).
[7]K. Inoue, F. Yano, A. Nishida, T. Tsunomura, T. Toyama, Y. Nagai, and M. Hasegawa, Appl. Phys. Lett. **93**, 133507 (2008).
[8]K. Inoue, F. Yano, A. Nishida, T. Tsunomura, T. Toyama, Y. Nagai, and M. Hasegawa, Appl. Phys. Lett. **92**, 103506 (2008).
[9]S. Koelling, M. Gilbert, J. Goossens, A. Hikavyy, O. Richard, and W. Vandervorst, Appl. Phys. Lett. **95**, 144106 (2009).
[10]Y. Shimizu, Y. Kawamura, M. Uematsu, K. M. Itoh, M. Tomita, M. Sasaki, H. Uchida, and M. Takahashi, J. Appl. Phys. **106**, 076102 (2009).
[11]E. Cadel, F. Vurpillot, R. Lardé, S. Duguay, and B. Deconihout, J. Appl. Phys. **106**, 044908 (2009).
[12]B. Gault, M. Müller, A. La Fontaine, M. P. Moody, A. Shariq, A. Cerezo, S. P. Ringer, and G. D. W. Smith, J. Appl. Phys. **108**, 044904 (2010).
[13]A. R. Waugh, E. D. Boyes, and M. J. Southon, Surf. Sci. **61**, 109 (1976).
[14]F. Vurpillot, A. Bostel, and D. Blavette, Appl. Phys. Lett. **76**, 3127 (2000).
[15]B. Gault, M. P. Moody, F. de Geuser, A. La Fontaine, L. T. Stephenson, D. Haley, and S. P. Ringer, Microsc. Microanal. **16**, 99 (2010).
[16]A. Shariq, S. Mutas, K. Wedderhoff, C. Klein, H. Hortenbach, S. Teichert, P. Kücher, and S. S. A. Gerstl, Ultramicroscopy **109**, 472 (2009).
[17]T. Kojima, R. Nebashi, K. M. Itoh, and Y. Shiraki, Appl. Phys. Lett. **83**, 2318 (2003).
[18]Y. Shimizu and K. M. Itoh, Thin Solid Films **508**, 160 (2006).
[19]Y. Shimizu, M. Uematsu, and K. M. Itoh, Phys. Rev. Lett. **98**, 095901 (2007).
[20]B. Gault, M. P. Moody, F. de Geuser, G. Tsafnat, A. La Fontaine, L. T. Stephenson, D. Haley, and S. P. Ringer, J. Appl. Phys. **105**, 034913 (2009).
[21]D. J. Larson, D. T. Foord, A. K. Petford-Long, H. Liew, M. G. Blamire, A. Cerezo, and G. D. W. Smith, Ultramicroscopy **79**, 287 (1999).
[22]P. Bas, A. Bostel, B. Deconihout, and D. Blavette, Appl. Surf. Sci. **87–88**, 298 (1995).
[23]B. Gault, D. Haley, F. de Geuser, M. P. Moody, E. A. Marquis, D. J. Larson, and B. P. Geiser, "Advances in the reconstruction of atom probe tomography data," Ultramicroscopy (to be published).
[24]Y. Shimizu, A. Takano, and K. M. Itoh, Appl. Surf. Sci. **255**, 1345 (2008).
[25]M. Tomita, H. Tanaka, M. Koike, S. Takeno, Y. Hori, and M. Takahashi, J. Vac. Sci. Technol. B **27**, 1844 (2009).
[26]M. G. Dowsett, R. D. Barlow, and P. N. Allen, J. Vac. Sci. Technol. B **12**, 186 (1994).
[27]M. Tomita, M. Koike, S. Takeno, Y. Kawamura, Y. Shimizu, M. Uematsu, and K. M. Itoh (unpublished).